Comparison of Different Water Tank Leg Cross Sections, when exposed to a Fire

Máté Petrik, Károly Jármai

Institute of Energy Engineering and Chemical Machinery, University of Miskolc, H-3515 Miskolc, Hungary
mate.petrik@uni-miskolc.hu; karoly.jarmai@uni-miskolc.hu

Abstract: The target of the investigation is a water tank with an internal volume of 1.5 m^3. This pressure vessel is supported by legs. This study compares four different cross sections of the support, when exposed to fire. Different steel grades were used for the comparison. During the fire, the temperature rises continuously, and with it, the yield strength of the steel decreases. The purpose of the calculation is to determine how long the structure can withstand buckling.

Keywords: pressure vessel support; fire load; buckling

1 Introduction

Relatively small water tanks are widely used in industry and households and usually supported by legs. These leg supports are very simple steel structures. They are usually a circular hollow section (CHS), rectangular hollow section (RHS) or I-section. Under normal operating conditions, the load on the leg support is due to the mass of the vessel and the liquid, which causes a compressive force. This means that the leg must be checked for buckling. The load on the bottom of the vessel in the support environment, which superposes the membrane stress state on the shell of the vessel, should be checked according to the EN 13445-3 standard.

In the case of fire exposure, two main features affect the temperature increase: The shape and the material of the leg support. The material properties (yield stress, Young modulus) required for the calculations decrease with increasing temperatures. In this present paper, different types of steel, structural and pressure steels have been investigated [1]. The other main parameter is the shape of the support, more specifically the ratio of the perimeter to the cross-sectional area.

Many researchers are involved in the investigation of the fire load of steel structures. Silva *et al.* [2] investigated an I-section using finite element method

(FEM) and compared the results for different fire loads (four-sided fire, three-sided fire). Xing *et al.* [3] investigated the local buckling mechanism of plates. Analytical and numerical calculations are established. Laím *et al.* [4] and Yang *et al.* [5] performed experiments on compressed columns. They both investigated cold-formed I-sections and demonstrated the typical failure mechanism with buckling modes during compression load.

2 Mechanical and Thermal Properties of the Steel Grades

2.1 Mechanical Properties

The two important mechanical properties in the heat transfer process are the yield strength and Young's modulus of the steel. These values are highly dependent on temperature, as shown in Figure 1.

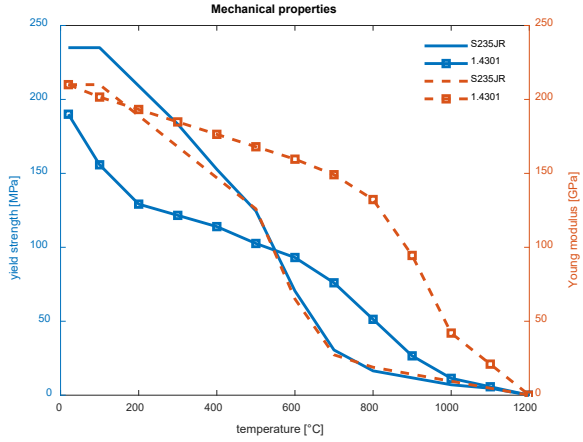

Figure 1
Temperature dependence of steel grades [6]

2.2 Thermal Properties

On the other hand, in this case not only the mechanical properties but also thermal properties, specific heat, density and thermal conductivity are important. These properties have a great influence on the heat transfer process; their values affect the rate of heating. In the solid state, temperature has no effect on density; its

value is constant at 7850 kg/m^3. However, specific heat and thermal conductivity highly dependent on temperature and microstructure [6]. The following graphs show the values of these two properties.

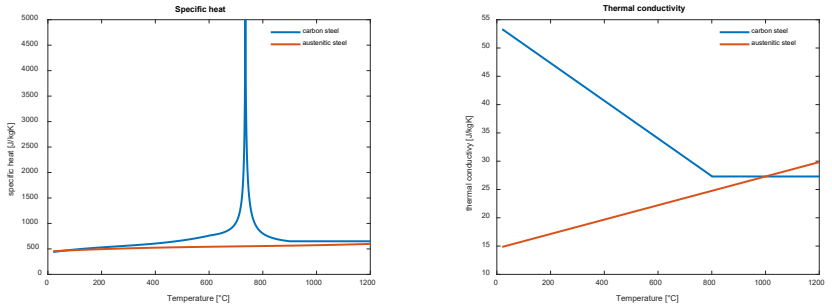

Figure 2
Temperature dependence of the thermal properties [6]

The specific heat graph shows that in the case of carbon steel, a phase transformation occurs in the steel structure and value of specific heat increases significantly near this temperature. This phenomenon slows down the heating of the legs. In the case of austenitic steel, there is no phase change and the value rises slightly as a function of temperature. The thermal conductivity also shows an interesting behavior. At room temperature, the thermal conductivity of carbon steel is more than 3,5 times higher than that of austenitic steel. However, as the temperature rises, the value of the carbon steel decreases, while that of austenitic will increases. Above 1000°C, the value of austenitic steel is higher. Both thermal properties have a strong influence on the temperature rise of the legs.

The value of the linear thermal expansion is an important material property for strength. In this case, the two grades of steel behave similarly, increasing in value with increasing temperature. Carbon steel has a value of 0.24 1/K and austenitic steel 0.33 1/K at room temperature. In this present study, this variation was not considered, since no additional collateral load from inhibited thermal expansion was assumed.

3 Thermal Calculation Method

The lumped heat capacity method was used to determine the duration of the load limit state (the value of time when the buckling occurs). In fire loading, heat from the fire is transferred to the structural material by convection and radiation. If the supports are facing the fire load and the vessel is also facing, the question may arise whether the bottom of the vessel should be checked. The high heat capacity

of the filled water causes the shell temperature to rise very slowly. The water cools the steel, so the present paper only deals with the buckling mechanism of the supports involved.

3.1 Convection and Radiation

In the case of fire loads, heat transfer is by convection and radiation. Since the velocity is negligible, an empirical Nu number correlation must be used to determine the convective heat transfer coefficient (α_c). However, the calculation is cumbersome and its value is almost neglectable when compared to the radiative heat transfer coefficient; this value is 20 W/m^{2}K according to the literature [7].

For the determination of the radiative heat transfer coefficient, which is much more decisive in this process, the modified form of Stefan-Boltzmann law is used, which is

$$\alpha_R(t) = \frac{\varepsilon_f \cdot \varepsilon_s}{\varepsilon_f + \varepsilon_s - \varepsilon_s \cdot \varepsilon_f} \cdot \sigma \left[T_f^2(t) + T_s^2(t) \right] \left[T_f(t) + T_s(t) \right], \tag{1}$$

where the different tags have the following meanings:

- ε_f is the emissivity of the fire [-], assuming 0.8
- ε_s is the emissivity of the surface of the support [-], assuming 1.0
- σ is the Stefan-Boltzmann constant ($5{,}67 \cdot 10^{-8}$ W/(m^{2}K^4))
- T_f is the temperature of the fire [K]
- T_s is the temperature of the leg support [K]

Eq. 1 shows that temperatures vary over time, but not in the same way. The fire temperature was determined using empirical correlation described in ISO 834 standard.

$$T_f(t) = 345 \cdot \log_{10}(8t + 1) + 20°\text{C} \tag{2}$$

In Eq. 2 the t time is given in minutes, and T temperature is given in °C. Based on these facts, the total heat flux from fire to legs is

$$\dot{q}(t) = \dot{q}_c(t) + \dot{q}_r(t) = \left[\alpha_c(t) + \alpha_r(t) \right] \cdot \left[T_f(t) - T_s(t) \right] \tag{3}$$

Each term in Eq. 3 depends on the time parameter. At lower temperatures the convective heat transfer method dominates, while at higher temperatures radiation can take orders of magnitude higher values.

3.2 Lumped Heat Capacity Method

Calculating the transient heat transfer can be difficult, especially for complex geometries. However, in the case of leg support, the cross-sectional area does not vary along its axis, so the complex method can be used. The simplification is based on comparing convection and radiation heat flux from fire to support and conduction through the wall. For this purpose, the heat transfer system is constructed in a similar way to an electrical network. There is a potential difference between the temperatures (analogous to the electrical voltage or potential), which indicates the heat flux from the higher temperature to the lower temperature (equivalent to electrical current). The proportional factor is the value of the resistance. The procedure described in the calculation is applicable when the Bi number, which is the ratio of the resistances, is less than 0.1 [7].

$$\mathrm{Bi} = \frac{R_{cond}}{R_{conv}} = \frac{s_{wall} / \lambda_{wall}}{1 / (\alpha_c + \alpha_r)} \tag{4}$$

In case when some sections are investigated, Eq. 4 changes to the following shape:

$$\mathrm{Bi} = \frac{(\alpha_c + \alpha_r) \cdot \frac{V}{A}}{\lambda_{wall}} \tag{5}$$

In Eq. 5, the *V/A* value is a section factor, which is the ratio of the cross-sectional area to the surface perimeter exposed to the fire.

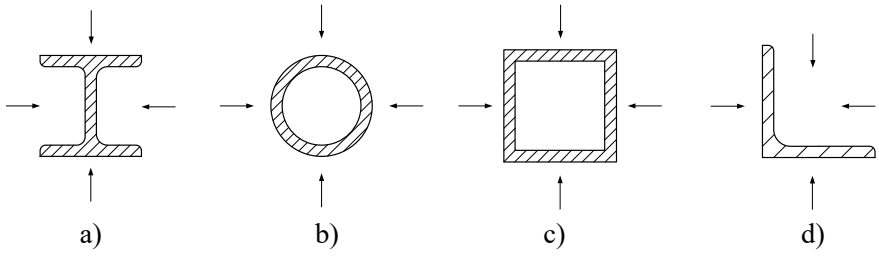

Figure 3

The investigated sections

a) I-beam, b) circular hollow section, c) square hollow section, d) hot rolled equal leg angles

Figure 3 shows the sections under consideration. All of them are standardized: DIN 1025 for I-beams, EN 10219-2 for circular and square hollow sections and EN 10056-1 for equal leg angles.

This Bi number must be less than 0.1. For a higher value, the outlined model cannot be applied. If the conditions are fulfilled, the average temperature increment of the investigated section can be calculated as follows:

$$\Delta T_s = \frac{\frac{A}{V}}{\rho_s \cdot c_{ps}} \cdot \dot{q} \cdot \Delta t, \tag{6}$$

where ρ_s is the density of steel [kg/m^3], c_s is the specific heat of steel [J/(kgK)], A/V is the section factor [1/m], $\dot{q}$ is the heat flux (calculated from Eq. 3), and Δt is the time step [s].

4 Thermal Calculation Method

When a compressive load is applied to a long and thin (or slender) rod, there is always a risk of buckling. The theory was developed initially by Euler (1778) to deal with this phenomenon and was extended by Tetmayer. The result of their research was the buckling curve shown in Figure 4.

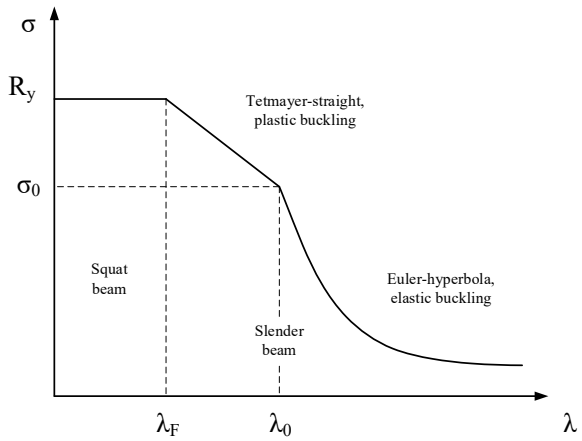

Figure 4
The buckling curve

The λ is the slenderness ratio and can be calculated in the equation below, describing the ratio between the length of the beam and the radius of gyration:

$$\lambda = \frac{K \cdot L}{r}, \tag{7}$$

where K is the effective length factor, describing the effect of the supports on buckling (L_0 often symbolized by the $K{\cdot}L$ product and represents the length of the beam after the buckling), σ_0 is the elastic limit stress, R_y is the yield strength of the steel. The radius of gyration is

$$r = \sqrt{\frac{I}{A}} \tag{8}$$

where I is the second moment of inertia of the cross-section, calculated according to the axis of the buckling, and A is the area of the cross-section.

The value of K can be seen in Figure 5.

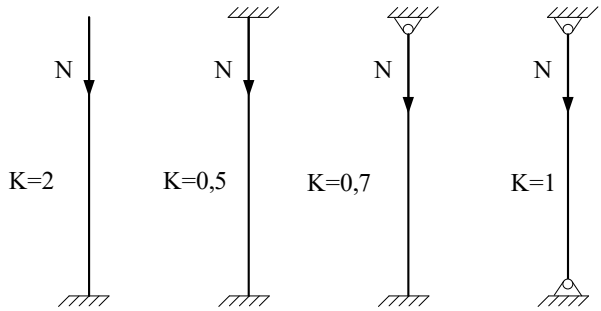

Figure 5
Buckling cases

The purpose of the calculation is to determine the value of σ_{limit} and compare it with the stress from the compressive load. The classical theory distinguishes two cases of plastic buckling, where the λ, in this case, is between λ_0 and λ_F:

$$\sigma_{\text{lim}} = a - b \cdot \lambda \tag{9}$$

where a and b are material constants. If the λ is above $\lambda_{0,}$ then the buckling is elastic, then the stress limit is

$$\sigma_{\text{lim}} = \left(\frac{\pi}{\lambda}\right)^2 \cdot E \tag{10}$$

where E is the Young's modulus of steel. The last possibility is when λ is below λ_F. In this case, the beam is stubby, there is no chance of buckling, and the limit stress is equal to the yield strength of the steel.

The classical theory assumes that the beam is perfectly straight, the cross-section is free from deformation, and the residual stress is 0. Nowadays, the buckling calculations are performed according to different standards, for example, Eurocode-3, JRA, API, AISC etc. In this study, calculations have been carried out according to Eurocode-3 part 1-1 (EN 1993.1.1-2005). This standard considers the effect on initial inaccuracy, the theory developed by Ayrton and Perry (1886), and the effect of the residual stresses from the welding, the theory developed by Beer and Schulz (1970). These were the first and the second additions to Euler's classical theory. The third and last addition was carried out by Maquoi and Rondal (1978), which resulted in a complex parameter describing the effect of initial curvature and residual stresses [8].

EC-3 classifies cross-sections into four classes; the curves are shown in Figure 6:

a) Welded I-beams, where f_y>420 MPa, and the flange plate thickness is less than 40 mm (Curve a_0)
b) Hot-formed hollow sections (Curve *a*)
c) Cold-formed hollow sections, welded box beams, and welded I-beams for buckling around the x-axis, if the flange plate thickness is less than 40 mm (Curve *b*)
d) Welded I-beams for buckling around the y-axis (this is the axis which is parallel to the web plate) when the flange plate thickness is less than 40 mm, and I-beams for buckling around the x-axis when the flange plate thickness is above 40 mm, moreover U, L and T beams and solid bars (Curve *c*)
e) Welded I-beams for buckling around the y-axis when the flange plate thickness is above 40 mm (Curve *d*)

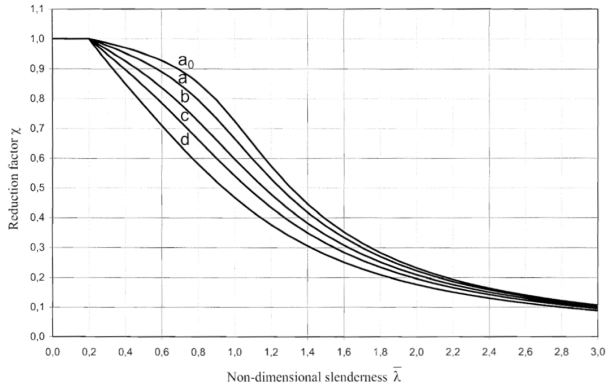

Figure 6
The reduction factor as a function of the slenderness ratio

The imperfection factor α is also given in Eurocode 3, and its value is shown in Table 1.

Table 1
The value of the imperfection factor

Buckling curve	a_0	*a*	*b*	*c*	*d*
Imperfection factor	0.13	0.21	0.34	0.49	0.76

For the leg supports, the Curve *c* applies, so the imperfection factor for the calculations is 0.49. Although the EN 1993-1-1 standard recommends Curve *b* for angle steels, this study used Curve *c* as a uniform curve due to the comparability of the significantly different geometries.

The following quantities should be introduced for the calculations:

$$\lambda_E = \pi \cdot \sqrt{\frac{E}{f_y}} \tag{11}$$

$$\bar{\lambda} = \frac{\lambda}{\lambda_E} \tag{12}$$

According to the standard, the next step is to calculate the factor Φ

$$\varphi = \frac{1}{2} \cdot \left[1 + \alpha \cdot \left(\bar{\lambda} - 0.2\right) + \bar{\lambda}^2\right]. \tag{13}$$

The buckling factor:

$$\chi = \frac{1}{\varphi + \sqrt{\varphi^2 - \bar{\lambda}^2}} \tag{14}$$

The inequality of the verification process:

$$\sigma = \frac{F}{A} \leq \chi \cdot f_y \tag{15}$$

The maximal value of χ is always 1, and if it is below 0.2, as χ=1, then the beam is squat, and there is no real possibility of buckling. The equations are valid for cross-section classes 1,2 and 3 but not for class 4. These classes are:

- Class 1: Those cross-sections which can form the plastic joint with the rotational capacity required by the plastic analysis without loss of the resistance.
- Class 2: Those cross-sections which are capable of forming their plastic moment capacity but have limited rotational capacity due to local buckling.
- Class 3: Cross-sections in which, assuming an elastic stress distribution, the stress in the extreme compressive strength of the steel structure can reach the yield strength, but local buckling may prevent the development of plastic moment resistance.
- Class 4: Cross-sections in which buckling occurs in one or more parts of the cross-section before reaching the yield point.

For cross-section Class 4, the effective area is used instead of A in equation (6). The calculation method is described in EN 1993.1.5 2006. The calculations are performed under the assumption that the stress can reach the yield point without local buckling.

4.2 Buckling during the Fire Load

In the calculations, the yield strength and Young's modulus must be calculated at a given temperature due to the fire load. Eurocode 3 does not give an exact value for the yield strength at a given temperature; instead, it uses a factor k multiplied

by the yield strength, which is given at 20 °C. The values of the factor are shown in Table 2 and are given in EN 1993.1.2.

Table 2
Values of the modification factors

Steel Temperature	The reduction factor for the yield strength of 1.4401 steel	The reduction factor of Young's modulus of 1.4401 steel	The reduction factor of the yield strength of carbon steel	The reduction factor of Young's modulus for carbon steel
20°C	1	0.05	1	1
100°C	0.88	0.049	1	1
200°C	0.76	0.047	0.807	0.9
300°C	0.71	0.045	0.613	0.8
400°C	0.66	0.03	0.42	0.7
500°C	0.63	0.025	0.36	0.6
600°C	0.61	0.02	0.18	0.31
700°C	0.51	0.02	0.075	0.13
800°C	0.4	0.02	0.05	0.09
900°C	0.19	0.02	0.0375	0.0675
1000°C	0.1	0.02	0.025	0.045

A linear interpolation between the values of the factors at a given temperature is used. The interpolation equation is as follows:

$$k_y = \frac{T - T_1}{T_2 - T_1} \cdot \left(k_{y2} - k_{y1}\right) + k_{y1} \tag{16}$$

In the equation, T is the temperature at which the calculation is made, and it is between T_1 and T_2. At these temperatures the yield strength and Young's modulus are given; these values are represented by k_{y1} and k_{y2}.

The buckling calculations with the reduction factor at the elevated temperature are as follows. The $\bar{\lambda}$ slenderness ratio at a given temperature is

$$\bar{\lambda}_T = \bar{\lambda} \cdot \sqrt{\frac{k_y}{k_E}} \tag{17}$$

where the $\bar{\lambda}$ is the slenderness ratio given by Eq. 10, k_y is the yield strength reduction factor, and the k_E is the reduction factor of the elastic modulus.

The α modification ratio (this is similar to the ε factor in case of buckling):

$$\alpha = 0.65 \cdot \sqrt{\frac{235\text{MPa}}{f_y}} \tag{18}$$

The reduced value of the factor φ:

$$\varphi_T = \frac{1}{2} \cdot \left(1 + \alpha \cdot \bar{\lambda}_T + \bar{\lambda}_T^2\right). \tag{19}$$

The modified reduction factor:

$$\chi_T = \frac{1}{\varphi_T + \sqrt{\varphi_T^2 - \bar{\lambda}_T^2}} \tag{20}$$

At elevated temperatures, the limit for buckling is as follows:

$$\sigma_T = \chi_T \cdot f_{y.} \cdot k_{y,\Theta} \tag{21}$$

This factor reduces the allowable stress on the support. This value is a function of the temperature, which is a function of time, just as the yield strength of steels is a function of temperature and time. The relationship between time and temperature is given by Eq. 2. When the two curves (yield strength-time and limit stress-time) cross, this point is the point of collapse due to the buckling.

5 Cases Studied and the Results

This section contains the results of the investigations. The lumped heat transfer analysis was set to the following functions:

- Material properties of the leg (which can be S235JR carbon steel grade or austenitic 1.4301 steel grade)
- Cross-section of the leg (shown in Figure 2)
- Geometric dimensions of the sections (diameter, height, width, wall thickness)

The length of the legs was the same, 1000 mm, and the diameter of the plate pads was also constant, at 140 mm. This present study compares the effect of the cross-section of the legs under fire load for a standard water vessel so that all other parts of the vessel are identical to not affect the results.

5.1 The Investigated Vessel

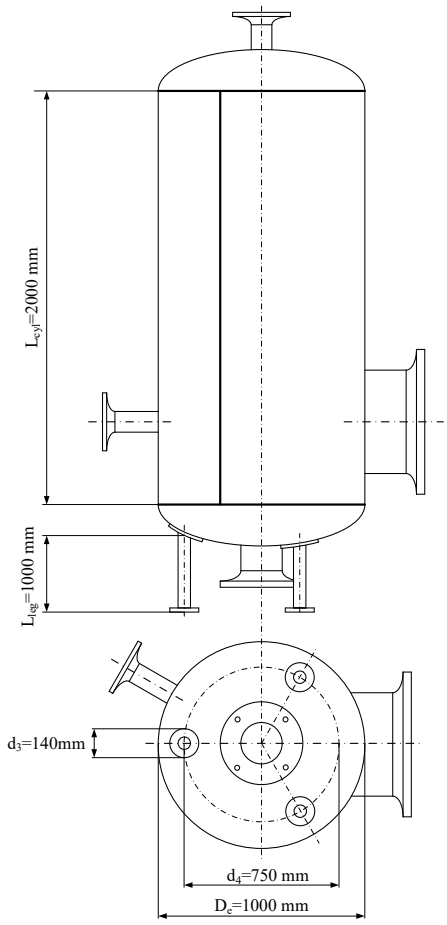

Figure 7
Schematic drawing of the investigated vessel

Figure 7 shows the geometric dimensions of the investigated water vessel. The vessel is made of P235GH steel grade, which is constant throughout the cases (and has no effect on the buckling of the legs). The external diameter is 1000 mm, the height is 2000 mm, the ends are thorispherical and are related to DIN 28011 standard, and the nominal wall thickness is 8 mm. With these data, the weight of the vessel is 550 kg, the volume of the vessel is 1.57 m^3, and the weight of the water is 1570 kg. While three legs were investigated, the force in one leg was 6935 N. This load was also constant for all leg cross-sections.

5.2 Results

5.2.1 Circular Hollow Sections

DN40 tube (Ø48.3x2.6 mm)

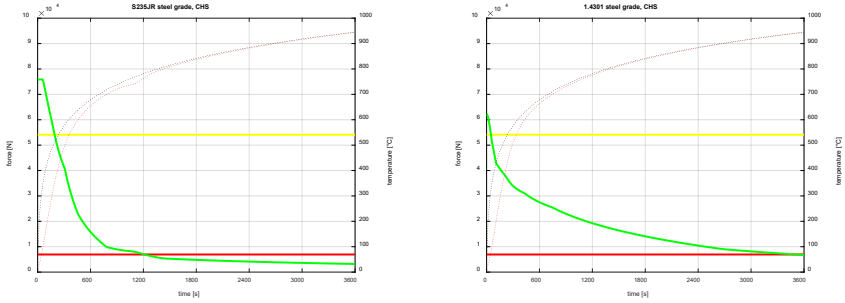

Figure 8
Force-time diagrams for DN40 tubes

DN50 tube (Ø60.3x2.9 mm)

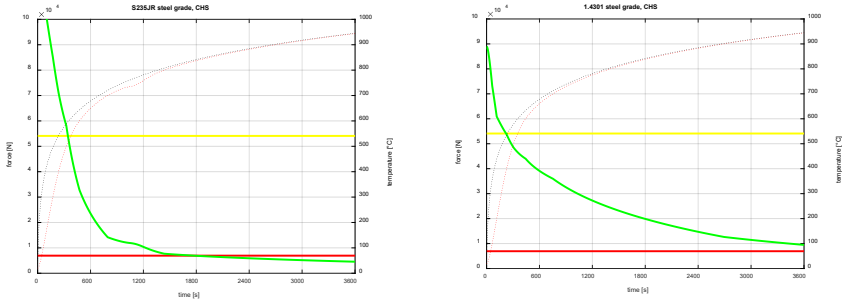

Figure 9
Force-time diagrams for DN50 tubes

DN65 tube (Ø76.1x2.9 mm)

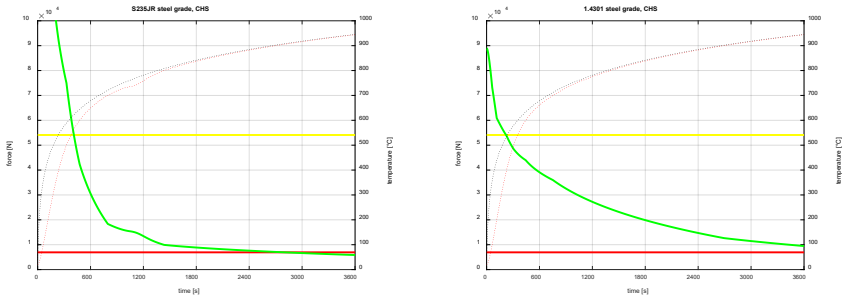

Figure 10
Force-time diagrams for DN65 tubes

5.2.2 Square Hollow Sections

40x2.5 mm

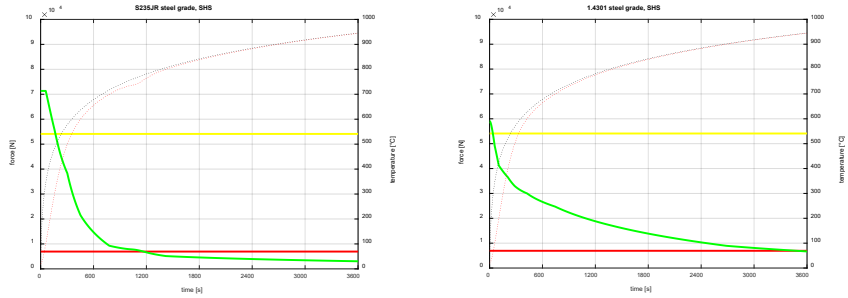

Figure 11
Force-time diagrams for 40x2.5 square hollow sections

50x2.5 mm

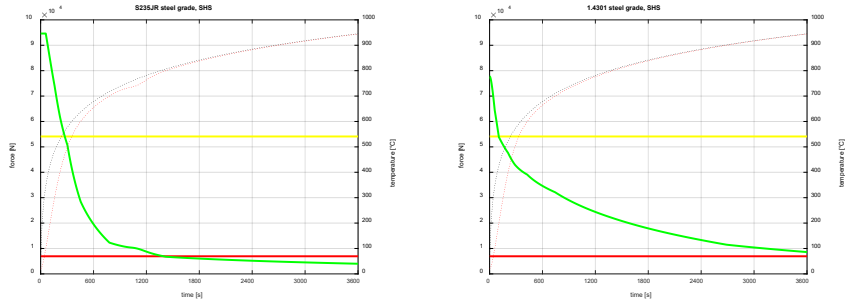

Figure 12
Force-time diagrams for 50x2.5 square hollow sections

60x2.5 mm

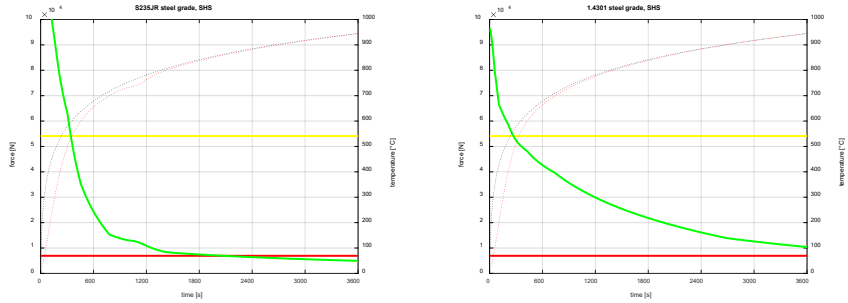

Figure 13
Force-time diagrams for 60x2.5 square hollow sections

5.2.3 Square Hollow Sections

I80 section

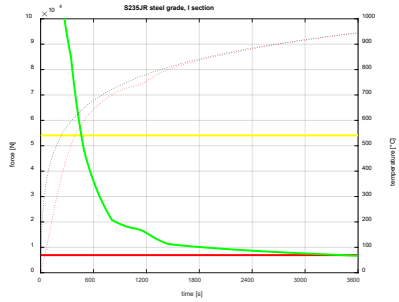

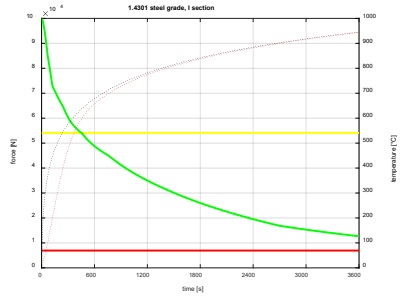

Figure 14
Force-time diagrams for I80 sections

I100 section

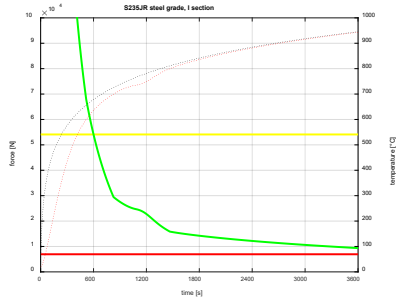

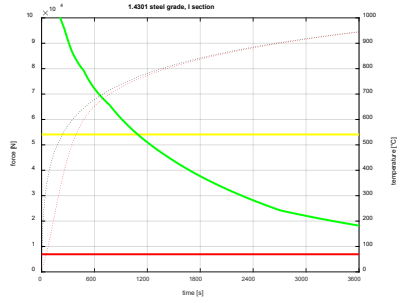

Figure 15
Force-time diagrams for I100 sections

5.2.4 Equal Leg Angles

35x4 mm

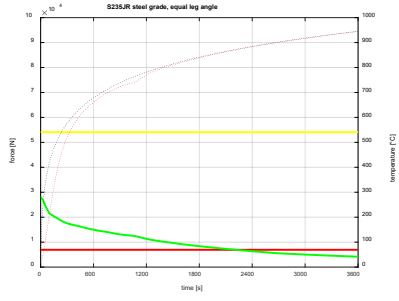

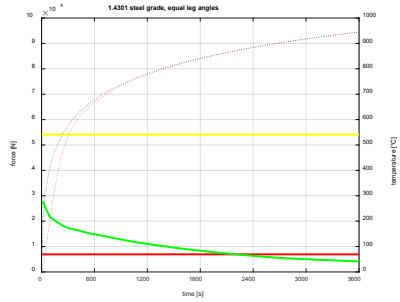

Figure 16
Force-time diagrams for 35x4 mm equal leg angles

40x4 mm

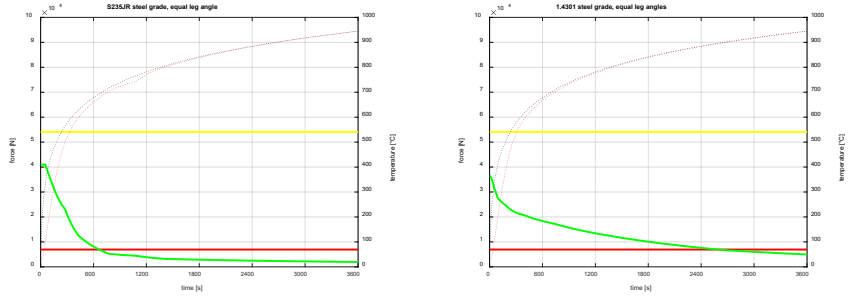

Figure 17
Force-time diagrams for 40x4 mm equal leg angles

45x4.5 mm

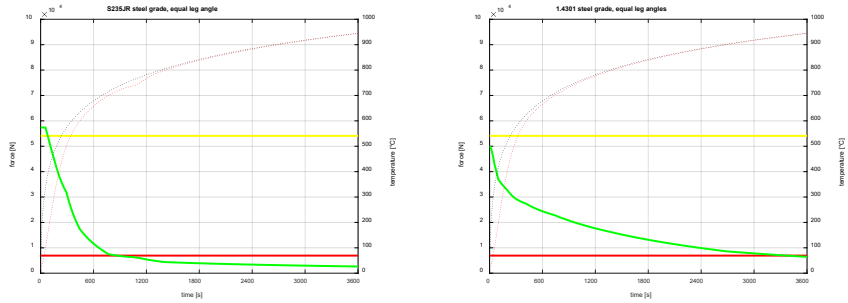

Figure 18
Force-time diagrams for 45x4.5 mm equal leg angles

60x5 mm

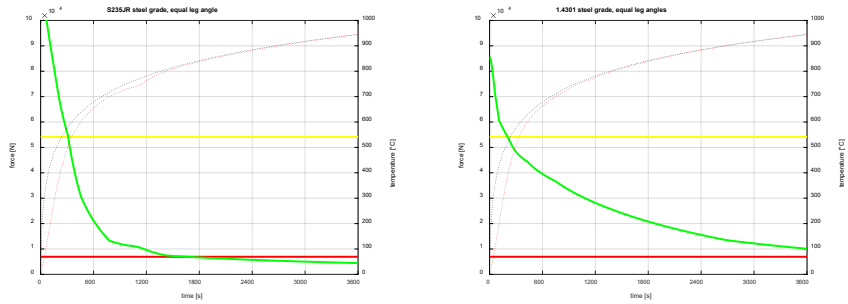

Figure 19
Force-time diagrams for 60x5 mm equal leg angles

From Figure 8 to Figure 19, the red lines are the forces in the legs, the yellow lines are the forces in the shell, and the green lines are the buckling limits. These belong to the left axis. The black dashed lines are the fire temperatures, the red dashed

lines are the temperature of the legs, and these belong to the right axis. It is clear from the figures that austenitic steels are preferable in all cases, but the use of this grade of steel is not recommended. This depends on the steel grade of the vessel. If the vessel is made of carbon steel, the reinforcing plate and the leg should also be made of carbon steel. In the case of austenitic vessels, both should also be austenitic. The explanation is the difficulty welding the two types of steel grade. Making a mixed carbon-austenitic weld is also difficult, and this weld will likely be the weak point of the device.

Furthermore, hollow sections are more favorable than open sections. This is because hollow sections have the smallest section factor, so that the temperature dependence will be the slowest in these hollow sections. The section factors will be much higher for I-sections or equal-leg sections. These will reach the buckling limit fastest. From Figures 14 and 15, I-sections seem to be the solution but note that they have a much larger cross-sectional area, as we used standard sections, of which these were the smallest. The following, Figure 20, simply compares these sections according to their degree of heating [9].

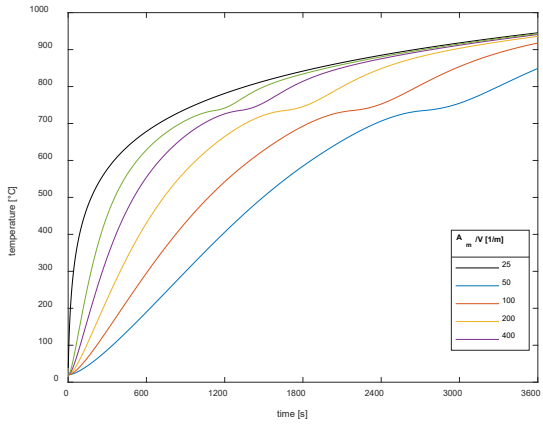

Figure 20
Comparison of section factors

5.2.5 Buckling Time

Figures 8-19 show the load on the legs, the buckling limit of the leg and the temperate of the fire and the leg support. At this point, the temperature of the vessel and the water in it were not calculated because the relatively high value of the specific heat of the water would cool the shell temperature. This 1-hour period is not long enough to cause considerable problems inside the vessel (high temperature, high value, phase change or BLEVE, which is the abbreviation for boiling liquid expanding vapor explosion). The following table shows the time interval at which the buckling occurred and the cross-section areas associated with them.

Table 3
Comparison of the buckling times

	S235JR	***1.4301***	***cross-section area***
CHS			
DN40	1214 s	3509 s	3.73 cm^2
DN50	1775 s	3600+ s	5.23 cm^2
DN65	2802 s	3600+ s	6.67 cm^2
SHS			
40x2.5	1166 s	3482 s	3.75 cm^2
50x2.5	1394 s	3600+ s	4.75 cm^2
60x2.5	2074 s	3600+ s	5.75 cm^2
I section			
I80	2291 s	3600+ s	7.57 cm^2
I100	3600+ s	3600+ s	10.6 cm^2
equal leg angle			
35x4	547 s	2207 s	2.67 cm^2
40x4	664 s	2596 s	3.08 cm^2
45x4.5	868 s	3371 s	3.9 cm^2
60x5	1655 s	3600+ s	5.82 cm^2

It is clear from Table 3 that austenitic steel is in all cases more favorable than carbon steel, even if the yield strength at room temperature is lower. In practice, CHS sections are the most commonly used, since the vessels are connected with pipelines and the leg support could be made from the remains of these pipes. I-section should be used for higher vessels and other steel structures, while equal leg angles are the weakest sections. By dividing the buckling time by the area of the cross-section for nearly equal cross-sections for carbon steel, the results are as follows.

Table 4
Comparison of the effectiveness of different sections

	CHS	***SHS***	***equal right angle***
section	DN50	60x2.5	60x5
t/A	339.42 s/cm^2	360.69 s/cm^2	284.36 s/cm^2

Conclusions

Based on the experimental study on different leg sections of the water tank exposed to elevated temperatures, as described earlier, the following conclusions can be drawn:

- The smaller the cross-sectional view factor examined, the slower the raw material heats up. This implies that the hollow sections are more favourable than the open sections and that the rate of heating can be reduced by the application of some protective material (paintings, hollow encasement, thermal insulation, and thermally foaming paint).

- In case of buckling, it does not matter how the foot was installed; it will bend along its weakest axis. In this respect, the circular hollow sections (CHS) and square hollow sections (SHS) are the best, as these do not have protruding axes.
- In the function of the steel structure, the temperature-dependent mechanical properties vary differently. In this respect, austenitic steels are much more suitable to withstand fire loading.
- Using the mathematical model presented, we can give a very accurate prediction of the expected failure. By drawing up a protection plan, we can guarantee which protection devices are recommended for fire penetration.

Acknowledgement

The research was supported by the Hungarian National Research, Development and Innovation Office under the project number K 134358.

References

[1] CEN, “Eurocode 3 : Design of steel structures - Part 1-1: General rules and rules for structures,” Eurocode 3, Vol. 1, No. 2005. p. 91 pp, 2005

[2] T. Silva, M. Carić, C. Couto, P. Vila Real, N. Lopes, and D. Skejic, “Buckling Analysis of Steel Frames Exposed to Natural Fire Scenarios,” Structures, Vol. 10, pp. 76-88, 2017

[3] Z. Xing, M. Kucukler, and L. Gardner, “Local buckling of stainless steel plates in fire,” Thin-Walled Struct., Vol. 148, No. November 2019, p. 106570, 2020

[4] L. Laím, H. D. Craveiro, R. Simões, A. Escudeiro, and A. Mota, “Experimental analysis of cold-formed steel columns with intermediate and edge stiffeners in fire,” Thin-Walled Struct., Vol. 146, No. February 2019, 2020

[5] J. Yang, W. Wang, Y. Shi, and L. Xu, “Experimental study on fire resistance of cold-formed steel built-up box columns,” Thin-Walled Struct., Vol. 147, No. May 2019, p. 106564, 2020

[6] CEN, “Eurocode 3: Design of steel structures - Part 1-2: General rules - Structural fire design,” Eurocode 3, Vol. 1, No. 2005. p. 20 pp, 2005

[7] C. Zhang and A. Usmani, “Heat transfer principles in thermal calculation of structures in fire,” Fire Saf. J., Vol. 78, pp. 85-95, 2015

[8] J. Farkas and K. Jármai, Analysis and Optimum Design of Metal Structures. Rotterdam, Hollandia: Balkema Publishers, 1997

[9] J. Farkas, “Nyomott körcsőszelvényű rúd optimális méretezése tűzállóságra,” Acélszerkezetek, vol. Különszám, pp. 13-16, 2008